

1 **Technical challenges and solutions in representing lakes**
2 **when using WRF in downscaling applications**

3 **M. S. Mallard^{1,*}, C. G. Nolte¹, T. L. Spero¹, O. R. Bullock¹, K. Alapaty¹, J. A.**
4 **Herwehe¹, J. Gula², and J. H. Bowden³**

5 [1]{National Exposure Research Laboratory, U.S. Environmental Protection Agency, Research
6 Triangle Park, North Carolina, USA }

7 [2]{Department of Atmospheric and Oceanic Sciences, University of California, Los Angeles,
8 California, USA }

9 [3]{Institute for the Environment, University of North Carolina, Chapel Hill, North Carolina,
10 USA }

11 *Currently at: Institute for the Environment, University of North Carolina, Chapel Hill, North
12 Carolina, USA

13 Correspondence to: M. S. Mallard (mmallard@email.unc.edu)

14 Revised manuscript: 21 January 2015

15
16 **Abstract**

17 The Weather Research and Forecasting (WRF) model is commonly used to make high resolution
18 future projections of regional climate by downscaling global climate model (GCM) outputs.

19 Because the GCM fields are typically at a much coarser spatial resolution than the target regional
20 downscaled fields, inland lakes are often poorly resolved in the driving global fields, if they are
21 resolved at all. In such an application, using WRF's default interpolation methods can result in
22 unrealistic lake temperatures and ice cover at inland water points. Prior studies have shown that
23 lake temperatures and ice cover impact the simulation of other surface variables, such as air
24 temperatures and precipitation, two fields that are often used in regional climate applications to
25 understand the impacts of climate change on human health and the environment. Here,
26 alternative methods for setting lake surface variables in WRF for downscaling simulations are
27 presented and contrasted.

28

29 **1 Introduction**

30 When using global climate model (GCM) fields to drive finer-scale regional climate model
31 (RCM) runs, typically the RCM does not have an oceanic or lake physics component and relies
32 on the GCM output to provide all water surface temperatures and ice cover. Within a
33 downscaling simulation, by design, the GCM is at a coarser spatial resolution than the RCM, so
34 inland water bodies in the region being simulated are either poorly resolved or not resolved by
35 the GCM. Prior to 2013, the Weather Research and Forecasting (WRF) model (Skamarock et al.,
36 2008) required exogenously prescribed water surface temperatures, as there was not capability to
37 prognosticate water temperatures. WRF has included an optional coupled ocean component
38 since version 3.5 was released in April 2013 (WRF User's Guide, 2014). Other RCMs have been
39 coupled to ocean models in order to simulate regions around the Arctic, Mediterranean Sea, and
40 Indian Ocean (e.g., Rinke et al., 2003; Ratnam et al., 2009; Artale et al., 2010; Gualdi et al.,
41 2013). However, when using WRF's default configuration, the sea surface temperature (SST)
42 fields used during the simulation are calculated from the driving data during the preprocessing
43 steps performed before WRF runs the simulation; during the model run, these prescribed water
44 temperatures are input at a user-specified frequency which is usually daily or sub-daily.
45 Similarly, lake surface temperatures (LSTs) and lake ice cover are prescribed by spatial
46 interpolation from the SST and sea ice fields in the driving data. In this study, we examine the
47 use of the Advanced Research WRF (Skamarock and Klemp, 2008) model applied as an RCM in
48 regions where the driving larger-scale data have a poor representation of lakes.

49

50 When the WRF Preprocessing System (WPS) interpolates skin temperatures from the coarser
51 global dataset (where both land and water temperatures are included in a single field), masks are
52 applied such that water temperatures from the GCM are used to set water temperatures on the
53 finer, target grid. Using the standard methods in WPS, interpolation is first attempted using 16
54 surrounding grid cells in the coarser grid; if this method fails due to a lack of the requisite 16
55 valid data points, WPS attempts other interpolation techniques using as many as four grid cells
56 and as few as one. While a full description of all WPS interpolation techniques is beyond the
57 scope of this study, more information is available in the WRF User's Guide (2014, p. 3-56 to 3-
58 59). When all other methods fail due to the lack of nearby water grid cells, WPS defaults to the
59 "search" approach, in which the nearest water point is used to set LSTs. When employing the

60 search option, water cells in the driving data are often distant from and unrepresentative of the
61 target cell in the WRF domain. The search option in WPS performs no interpolation or
62 averaging, sometimes resulting in abrupt, non-physical temperature discontinuities.

63

64 Here we show the result of using this default methodology to downscale 1° Community Earth
65 System Model (CESM) fields to a 36 km WRF domain (198 × 126) covering the continental US,
66 and subsequently similar examples in other downscaling studies are discussed. However, it
67 should be noted that the use of CESM as an example is arbitrary because similar results have
68 been obtained with other global datasets as well. The CESM ocean mask, used to interpolate the
69 GCM's SST fields to the WRF grid, has no water grid cells over the North American interior
70 (Fig. 1). As a result, water temperatures in Hudson Bay are used to set temperatures over the
71 larger westernmost areas of the Laurentian Great Lakes, while LSTs in the southeastern areas of
72 the Great Lakes are set by Atlantic SSTs (Fig. 2). At the time shown in Fig. 2, the LSTs
73 interpolated from CESM onto the 36 km WRF grid contain discontinuities of approximately 17
74 K between adjacent grid cells in Lakes Michigan and Huron, while a smaller discontinuity of
75 approximately 3 K is created in Lake Superior. It should be noted that various interpolation
76 options are available in WPS and can be specified by the user. The description in the paragraph
77 above is representative of the interpolation process as defined by WPS's default settings. Even
78 though this process could be changed by the model user, the key issue remains that when lakes
79 are poorly represented or completely absent, the problem of how to specify the lake state is not
80 amenable to any interpolation method.

81

82 The problems of using larger-scale data to define LSTs with the default options in WPS are not
83 limited to the Great Lakes. None of the inland lakes resolved by WRF at 36 km have valid LSTs
84 in the CESM ocean mask (Fig. 1). Using the search option in WPS results in setting the LSTs to
85 unrealistic values throughout the domain. Temperatures in Pyramid Lake, Great Salt Lake, as
86 well as several smaller lakes east of the Rocky Mountains in both Canada and the US are
87 assigned from the Pacific Ocean (Fig. 2), while lake temperatures in the southeastern and central
88 US are set from SSTs in the Gulf of Mexico and Atlantic Ocean. Two adjacent grid cells
89 representing Lake Sakakawea in North Dakota are assigned LSTs differing by approximately 10
90 K because the western cell is set from the Pacific while the eastern cell is prescribed from

91 Hudson Bay (Fig. 2). Using any interpolation method to assign LSTs when no suitable data are
92 available will adversely affect the accuracy of downscaled simulations that are based on forcing
93 from those LSTs.

94

95 Mallard et al. (2014; hereafter M14) also discuss problems that arise when downscaling coarse
96 global data to a 12 km grid covering the eastern US. In M14, the National Centers for
97 Environmental Prediction (NCEP)–Department of Energy Atmospheric Model Intercomparison
98 Project (AMIP-II) reanalysis (hereafter R2; Kanamitsu et al., 2002) is used to drive historical
99 simulations as a proxy or stand-in for a similarly-coarse GCM. In contrast to the CESM example
100 discussed above, R2 has at least a partial representation of western Great Lakes, but nevertheless
101 has only three inland water points to represent all five of the Great Lakes (Fig. 1 of M14).

102 Therefore, using the standard interpolation methods with R2 results in unrealistically large,
103 abrupt, and non-physical LST discontinuities in eastern Lake Erie and Lake Ontario, where water
104 temperatures are set using Atlantic SSTs, while the LSTs in western Lake Erie and in the three
105 western Great Lakes are interpolated from the three lake cells in R2 (M14).

106

107 In WRF, ice cover can either be interpolated from the driving data and assigned to cover some
108 fraction of a grid cell, or it can be treated as a binary field that is set to 100 % at grid cells where
109 the water surface temperature drops below a specified threshold. The default threshold value was
110 271 K (slightly below the freshwater freezing temperature of approximately 273 K), but it was
111 changed to 100 K as of version 3.5.1 to avoid the unintended creation of ice by this method
112 when using WRF's default settings (Table 1). When fractional ice values are prescribed from the
113 driving dataset, the WPS methods applied to interpolate sea and lake ice differ from those used
114 for SSTs and LSTs. If there are no surrounding water grid cells in the driving dataset, an ice
115 cover value of zero is assigned rather than employing the search method. When M14 downscaled
116 ice cover from R2, it was shown ice concentrations of zero were applied to points through Lakes
117 Huron, Erie and Ontario throughout a two-year simulation (Fig. 3 of M14), even though partial
118 ice coverage was observed on all three lakes during that historical period. Moreover, almost
119 complete ice coverage of Lakes Superior and Michigan occurred in a single day (M14). Wang et
120 al. (2012a) conducted a climatology of ice cover in the Great Lakes over the period 1973 to 2010
121 and showed that, in the average seasonal cycle of ice cover, the maximum fractional coverage of

122 Lake Superior was approximately 50 % (their Fig. 3). Although Wang et al. noted that the
123 standard deviation of ice cover is quite large (exceeding the mean values in some of the Great
124 Lakes), the seasonal cycles in their study showed the accumulation of ice coverage over months,
125 not the abrupt appearance of lake-wide ice over daily periods. Ultimately, M14 improved the
126 representation of the Great Lakes in their downscaled simulations by applying a coupled lake
127 model, which will be discussed further in a subsequent section. Whereas M14 showed the results
128 of using a single lake model, the current work presents a broader range of approaches,
129 recognizing that the most preferable method to represent lake fields may vary between different
130 RCM applications.

131
132 Prior studies downscaling other global datasets and GCMs have also noted findings similar to the
133 example shown here (Fig. 2) and the results of M14. Using WRF as an RCM over Eastern
134 Africa, Argent (2014) showed that the use of WPS's default interpolation methods resulted in
135 oceanic temperatures from a global SST dataset applied to set LSTs throughout Lake Victoria.
136 Discontinuities in LSTs with WRF were noted in the Great Lakes basin by Bullock et al. (2014)
137 who downscaled R2 to 12 km, and by Gao et al. (2012) who downscaled CESM to a 4 km grid.
138 Within the downscaled simulations produced for the North American Regional Climate Change
139 Assessment Program (NARCCAP; Mearns et al., 2012), problems with producing realistic LSTs
140 and ice cover for the Great Lakes region are documented using several approaches with various
141 RCMs, including WRF (NARCCAP, 2014). For some NARCCAP model configurations, caution
142 is recommended when using surface variables in the region surrounding the Great Lakes.
143 Previous work examining the value of dynamical downscaling has noted that downscaled
144 simulations have the most potential to add value relative to GCM simulations in areas of
145 complex topography and along coastlines because of increased resolution in regional models
146 (e.g., Feser et al., 2011). Although RCMs better resolve the coastlines (and therefore, the
147 presence of lakes) than the driving GCMs, using erroneous LSTs and lake ice cover could impair
148 the simulation of interactions between lakes and overlying air masses. The potential benefits
149 gained by downscaling to a grid spacing that better resolves land–water interfaces may not be
150 realized if the lake state (defined here by LSTs and ice) is unrealistically represented. Even as
151 additional computing resources allow GCMs to increase in resolution and better represent lakes,
152 RCMs will also be run at finer scales; therefore, it can be expected that smaller lakes with

153 important effects on mesoscale and microscale climatology will continue to be unresolved by the
154 driving data sets.

155

156 The purposes of this paper are to describe various techniques that can be used to set LSTs and
157 lake ice cover in the WRF model for downscaling, and to discuss the benefits and possible
158 shortcomings of each approach. The effects of these techniques on simulated lake–atmosphere
159 interactions, both in the present climate and in future climate states, are discussed in context with
160 relevant previous literature.

161

162 **2 Comparison of methods**

163 As will be shown below, choice of the appropriate methodology for representing a lake in a
164 downscaling configuration is dependent on what interactions must be simulated between the
165 atmospheric fields and the lake state and how the lake state is expected to be impacted by climate
166 change when downscaling future GCM projections. In regional climate simulations conducted
167 over the continental US, the Laurentian Great Lakes are a prominent feature, as Lake Superior is
168 the largest freshwater lake in the world (by surface area) at over 82 000 km². Several studies
169 have concluded that the Great Lakes strongly influence the surrounding regional climate,
170 moderating extremes in near-surface temperatures, and affecting precipitation and passing
171 cyclones and anticyclones on an annual cycle (e.g., Wilson, 1977; Bates et al., 1993; Scott and
172 Huff, 1996; Notaro et al., 2013). Climatologically, the greater heat capacity of the lakes serves to
173 enhance precipitation and convection during September to March, when warmer surface water
174 (relative to low-level atmospheric temperatures) reduces atmospheric stability (e.g., Notaro et al.,
175 2013). Conversely, the slower warming of the lakes in boreal spring results in the opposite effect
176 during the April–August period, where the relatively cool lakes enhance atmospheric stability
177 and reduce precipitation and convection. These periods are referred to as the lake unstable and
178 lake stable seasons, respectively. Lake-effect precipitation has also been documented outside the
179 Great Lakes as well, such as in Lake Champlain (Tardy, 2000; Laird et al., 2009), Lake Tahoe
180 (Cairns et al., 2001), and the Great Salt Lake (Carpenter, 1993; Steenburgh and Onton, 2001). A
181 review by Schultz et al. (2004) states that lake-effect snowfall has been observed to occur over
182 lakes with fetches of only 30 to 50 km, citing prior studies over Bull Shoals Lake of Arkansas
183 (Wilken, 1997) as well as Lake Tahoe and Pyramid Lake in Nevada (Cairns et al., 2001; Huggins

184 et al., 2001). Interactions between the lakes and surrounding regions are also strong in tropical
185 environments as well. For example, the immediate region surrounding Lake Victoria in Africa
186 has the highest recorded frequency of thunderstorms in the world with approximately 300 storm
187 days per year (Asnani, 1993). Overall, while a comprehensive review of the impact of each lake
188 on regional climate is beyond the scope of this study, prior work indicates that even lakes that are
189 smaller than the Great Lakes can be anticipated to have substantial effects on regional climate.

190

191 Prior studies have also illustrated that even relatively small errors in prescribed LSTs in a
192 downscaling configuration can adversely affect simulated precipitation in regions surrounding
193 lakes. The sensitivity study of Wright et al. (2013) showed significant changes in lake-effect
194 snowfall over the Great Lakes in idealized simulations where LSTs were uniformly warmed by 3
195 °C. Anyah and Semazzi (2004) simulated changes in the spatial patterns and intensity of
196 precipitation, as well as the amount of evaporation, over Lake Victoria in a modeling study
197 where LSTs were uniformly changed by only 1.5 °C.

198

199 Interactions between the lakes and overlying air masses are also governed by the amount of lake
200 ice in climates that permit lakes to freeze. Previous studies have found the presence of ice
201 suppresses turbulent latent and sensible heat fluxes from the lake to the air mass (e.g., Zulauf and
202 Krueger, 2003; Gerbush et al., 2008). As shown in the lake-effect snow case studies simulated by
203 Wright et al. (2013), the presence of ice coverage over the lake's surface inhibits downstream
204 precipitation. As a result, lake-effect snowfall decreases in some areas surrounding the Great
205 Lakes during the later portion of the lake unstable season, as the water's surface freezes during
206 the winter and early spring months. Overall, past studies indicate that if LSTs and ice are not
207 properly prescribed, inaccurate values of precipitation and temperature in the lee of lakes result
208 from a downscaled simulation.

209

210 **2.1 WRF's alternative lake setting**

211 Since the release of WRF version 3.3 in April 2011, an "alternative initialization of lake SSTs"
212 option is provided in WPS to set LSTs (WRF User's Guide, 2014; Table 1). When employing
213 this method, LSTs can be set using temporally averaged 2 m air temperatures from the driving

214 data set, with the averaging period set by the user. Bullock et al. (2014), when downscaling a
215 proxy GCM (R2) over a 12 km grid covering the Great Lakes, attempted to use the alternative
216 lake setting to account for the greater thermal inertia of the Great Lakes by incorporating
217 seasonal temperature changes after a one-month time lag. Following the procedure of Bullock et
218 al., if a user were to perform a simulation over the month of May, a single LST field would first
219 be generated by temporally averaging air temperatures during the previous month of April;
220 subsequently this static LST field would be used to set inland water temperatures throughout the
221 month of May. Because Bullock et al. (2014) preprocessed the driving data in monthly segments,
222 the LST field was prescribed to vary with time on a monthly basis. Using this method may
223 imitate the seasonal changes observed over the Great Lakes, producing a lake stable and unstable
224 season during the appropriate months. A drawback to this methodology is that the same lag time
225 is used throughout the model grid, regardless of lake depth. Therefore, in this approach, large,
226 deep lakes are implied to heat and cool on the same timescale as small, shallow lakes.
227 Meanwhile, it is expected that observed seasonal temperature changes over smaller and
228 shallower lakes would more closely follow atmospheric temperature changes than in large, deep
229 lakes. If employed for simulations outside the Great Lakes, the procedure used by Bullock et al.
230 (2014) should be modified to imitate the observed relationship between changing air
231 temperatures and LSTs.

232
233 In its default configuration used prior to the release of version 3.5.1, WRF prescribes ice cover at
234 grid cells where LST is less than 271 K (Table 1). This value is applied at all water points
235 regardless of salinity. As winter 2 m air temperatures are frequently below freezing in the Great
236 Lakes area, Bullock et al. (2014) found that unrealistically large spatial coverage of ice occurred
237 when using the alternative lake setting in WRF version 3.4.1, with all five Great Lakes
238 completely frozen for most of the winter. Such erroneous ice cover would be expected to
239 negatively impact the simulation of precipitation, 2 m temperatures, and other variables
240 influenced by sensible and latent heat fluxes supplied by the Great Lakes. Therefore, the use of
241 the alternative lake setting in WRF may not be appropriate in some regions where sub-freezing
242 air temperatures would result in unrealistic temporal and spatial coverage of sub-freezing LSTs
243 and ice.

244

245 However, this is not a concern for tropical lakes where air temperatures would not be sufficiently
246 low enough to result in frozen lakes. Argent (2014, Sect. 3) demonstrated the utility of the
247 alternative lake setting in WRF simulations over Lake Victoria in Eastern Africa, finding that it
248 improved the accuracy of simulated rainfall relative to the use of the default interpolation in
249 which oceanic SSTs were used to set Lake Victoria's LSTs.

250

251 **2.2 Climatological LSTs and ice**

252 Another approach for setting LSTs and lake ice coverage when downscaling with WRF is to
253 prescribe these variables from higher-resolution data sets of climatologically averaged quantities.
254 This can be viewed as assuming stationarity for the lake state as is frequently done for other
255 input variables in an RCM, such as land-use and vegetation. Even for retrospective climate
256 simulations, using this approach could be detrimental because the interannual variability of LSTs
257 and ice – and its effects on the prediction of extreme events – would not be captured using this
258 method. When making future projections, it must be considered that prior studies have shown
259 that LSTs cannot be assumed to be stationary in future warmer climates; in fact, some studies
260 conclude that non-linear feedbacks exist between regional climate change and LSTs and ice for
261 some lakes. An observational study by Austin and Colman (2007) found that the multi-decadal
262 warming trend in the Great Lakes region was amplified in the lake temperatures, relative to
263 surrounding inland temperatures, because of the earlier break-up of ice and earlier springtime
264 warming of surface water. In the downscaling simulations of Gula and Peltier (2012), increased
265 snowfall was simulated in the lee of the Great Lakes in a warmer, mid-century climate because
266 lake ice forms later in the winter. Gula and Peltier conclude that the impact of having the lakes
267 remain free of ice is that increased latent and sensible heat fluxes are present for a longer time
268 period during the lake unstable season, lessening the stability of the overlying air mass and
269 enhancing precipitation. Magnuson (2000) concluded that observed ice coverage is decreasing in
270 lakes and rivers throughout the Northern Hemisphere. Such a decrease in ice coverage has been
271 linked by observational studies to increases in lake-effect precipitation in the Great Lakes region
272 (Assel and Robertson, 1995; Burnett et al., 2003; Kunkel et al., 2009). Because ice suppresses
273 fluxes of latent and sensible heat (e.g., Zulauf and Krueger, 2003; Gerbush et al., 2008),
274 decreasing ice cover in a warmer climate allows larger fluxes of latent and sensible heat to

275 modify the overlying air mass, increasing downstream precipitation during the lake unstable
276 season. None of the impacts on the lake state reviewed here (the warming of LSTs and more
277 open water from which to produce fluxes) would be considered in the WRF model using LSTs
278 and ice based on present-day climatology, and the effects of changing lake conditions on
279 atmospheric stability, humidity, precipitation and convection would not be simulated.

280

281 This approach could be improved by adding a linear increase to observed LSTs over time, which
282 may be a valid approximation for the effect of climate change on some lakes. However, such an
283 approach would not capture the non-linear impacts of climate change (as described by Austin
284 and Colman, 2007) on the Great Lakes. Overall, the efficacy of using of a climatologically-based
285 approach is dependent on the amount of interannual variability, as well as the impacts of climate
286 change on the lake state and whether those effects can be accounted for by the inclusion of a
287 linear LST anomaly.

288

289 **2.3 Land mask modification**

290 To avoid the issues with LSTs discussed in Sect. 1 and illustrated in Fig. 2, Gao et al. (2012)
291 modified the GCM land mask in the Great Lakes area so that skin temperatures from land points
292 in the GCM were used to set LSTs on the WRF grid in their downscaled simulations. This
293 treatment successfully eliminated the abrupt temperature discontinuities (such as those in Fig. 2)
294 produced by interpolating a coarse data set. However, the effects of the lakes themselves are lost
295 if GCM land temperatures are used to prescribe RCM water temperatures and the lake-land
296 temperature contrasts, with their associated mesoscale phenomena such as lake breezes and lake-
297 effect precipitation, are eliminated. Notaro et al. (2013) conducted an idealized modeling
298 experiment where the Great Lakes were replaced with forest and field land cover types. They
299 found that the presence of the lakes affected precipitation, 2 m air temperatures and their
300 variability, water vapor, cloud cover, incoming shortwave radiation, the hydrological budget and
301 the intensity of passing cyclones and anticyclones. The approach used by Gao et al. (2012),
302 where land surface temperatures from the GCM are used to specify water temperatures, partially
303 accounts for some lake effects (such as changes in surface friction and albedo) because WRF
304 would recognize the presence of a water surface. However, all processes related to the LST (e.g.,

305 ice formation, latent and sensible heat flux, 2 m temperature and moisture values, outgoing
306 longwave radiation from the surface) would be negatively impacted by this treatment.
307 Additionally, some impacts of climate change on the future lake state could be lost. For example,
308 the amplification of Great Lakes LSTs, relative to over-land temperatures, observed by Austin
309 and Colman (2007) will not be captured if land temperatures are used to set LSTs.
310

311 **2.4 Use of simulated lake fields from GCM**

312 A more sophisticated class of approaches for better representing the lake state in a downscaling
313 configuration involves the use of a lake model. This can be done either by using outputs from the
314 GCM's lake model (if available), driving a stand-alone lake model offline with GCM fields to
315 simulate LSTs and ice, or by coupling a lake model to the RCM when downscaling. The CESM
316 has a lake model embedded within its land surface model (LSM), version 4 of the Community
317 Land Model (CLM4). CLM4 accounts for the presence of subgrid-scale lakes using the one-
318 dimensional lake model described in Oleson et al. (2010). It is a column model partially based on
319 the Hostetler lake model (e.g., Hostetler and Bartlein, 1990; Hostetler et al., 1993, 1994), and it
320 simulates 10 water layers through the depth of the lake, as well as additional layers for
321 thermally-active soil underneath and snow and ice above. However, when producing the
322 downscaled simulation shown in Fig. 2, output from CLM's lake model was not easily accessible
323 with other CESM outputs from the same simulation within archiving systems such as the Earth
324 System Grid Federation. Lake temperatures and ice from CESM, and other GCMs with
325 embedded lake models, could be leveraged by RCMs such as WRF to account for the impact of
326 climate change on the lake state. In areas where lakes are at least partially resolved by the GCM,
327 this approach would be effective at driving the RCM with simulated changes in LSTs and ice
328 cover consistent with future projections and at keeping the RCM solution in the regions affected
329 by lakes consistent with the GCM simulation. However, some small lakes may remain
330 unrepresented by GCM data.
331

332 **2.5 Use of a stand-alone lake model**

333 If lake model outputs from the GCM are unavailable, one alternative is to use a standalone lake
334 model driven by GCM fields to downscale the lake state in a manner which is consistent with the
335 GCM's atmospheric fields. In the downscaling experiments performed by Gula and Peltier
336 (2012) over the period 2050–2060, the Freshwater Lake (FLake) model was utilized to provide
337 simulated LSTs and lake ice to WRF in the Great Lakes basin. GCM fields from the Community
338 Climate System Model, with a spectral resolution of T85 (~ 1.4° grid spacing), were used to
339 drive a FLake simulation on a 10 km regional grid, and the LSTs and ice cover simulated by
340 FLake were subsequently used to drive the downscaled WRF simulation. In this 1-way WRF-
341 FLake model configuration, changes in LSTs and ice respond to changes in atmospheric
342 variables in the driving GCM, but the lake model output is produced on the higher-resolution
343 regional WRF grid. FLake is a 1-D column model which is highly reliant on empirical
344 relationships and has been used in several studies with other RCMs (e.g., Mironov, 2008;
345 Kourzeneva et al., 2008; Martynov et al., 2008; Mironov et al., 2010; Samuelsson et al., 2010).
346 FLake requires a 2-D field of lake depths and the 1-D column model is called at each point.
347 Therefore, the simulated LSTs are sensitive to lake depth, as well as the driving GCM fields.
348

349 **2.6 Use of a coupled lake model within an RCM**

350 In WRF version 3.6 a CLM-based lake model can be utilized with other non-CLM land surface
351 models (WRF User's Guide, 2014; Table 1). This lake model is taken from CLM version 4.5
352 (Subin et al., 2012; Oleson et al., 2013) with some modifications by Gu et al. (2013) as discussed
353 further below. Although a version of CLM4 was available as an LSM option within WRF
354 version 3.5, the lake model in CLM4 was disabled in WRF (Table 1). In WRF version 3.6,
355 CLM's Hostetler-based lake model can be applied by using horizontally varying lake depths
356 (which are available in WPS version 3.6) or a uniform lake depth can be assigned to all lakes at
357 runtime. Gu et al. (2013) demonstrated WRF-CLM's performance in the Great Lakes region
358 using a previous version of this model configuration (WRF 3.2 and CLM 3.5) to simulate a 16
359 month period from 2001 to 2002 at 10 km grid spacing. It was shown that the lake model
360 simulated LSTs well in Lake Erie but generated large biases in LSTs when compared to buoy
361 observations in Lake Superior. However, the LST bias was reduced by reformulating the eddy

362 diffusivity parameter in the CLM lake model, and it was concluded that the updated lake model
363 within WRF-CLM was reasonably able to reproduce observed LSTs. However, no ice was
364 observed during the period and the ability of WRF-CLM to accurately simulate ice cover was not
365 examined in Gu et al. (2013).

366
367 In an alternative coupled approach, the prior work of Gula and Peltier (2012) has been updated
368 with the option of using WRF-FLake as a 2-way coupled model, where atmospheric variables
369 simulated by WRF are used by FLake at each time step in the WRF model, and simulated LSTs
370 and ice thicknesses are provided back to WRF by FLake. M14 concluded that the use of WRF-
371 FLake resulted in a more accurate representation of LSTs and lake ice, relative to interpolation
372 from the R2. Substantial improvements were shown in the simulation of the temporal and spatial
373 variability of ice cover, and errors in LSTs were reduced by the use of the coupled model.
374 Similar to Martynov et al. (2010), M14 found that FLake performed worst in the largest and
375 deepest lake (Lake Superior) and best for the smallest and shallowest (Lake Erie).

376
377 When using an embedded lake model within an RCM, it can be anticipated that the period of
378 time needed for spin-up could be larger than it is when all water conditions are simply
379 prescribed. To spin-up the WRF-FLake model in M14, the stand-alone version of the FLake
380 model was driven with atmospheric conditions from the proxy GCM in a spin-up procedure
381 recommended by Mironov et al. (2010) when using FLake. In this methodology, the initial year
382 of the simulation is “looped” over 10 annual cycles with meteorological variables from the
383 initial year repeatedly used to force the lake model, and the lake state at the end of each year
384 used to initialize FLake for the start of the next year, ensuring that the simulated lake state
385 converges to equilibrium with these atmospheric conditions by the end of the 10-cycle
386 simulation. Output from the first year of this offline simulation is shown in Fig. 3 illustrating the
387 adverse effects of using FLake output without adequate spin-up time. A time series taken from a
388 representative point in Lake Superior shows unrealistically cool LSTs (below 200 K) occurring
389 during the initial months of the simulation. Also during this period, unrealistically large ice
390 coverage formed, freezing over all five Great Lakes. The observed ice cover plotted in Fig. 3 is
391 much more limited in its spatial extent. Observed ice cover is plotted from National Ice Center
392 (NIC) ice charts, which are processed and provided by the Great Lakes Environmental Research

393 Laboratory (GLERL; Wang et al., 2012b). The FLake model results obtained after the spin-up
394 period showed realistic values of LSTs and ice cover (M14).

395
396 To examine how WRF-CLM reacts during the initial months of a simulation, without any spin-
397 up time, output from a 12 km WRF-CLM simulation (version 3.6) is shown in Fig. 4. In this
398 simulation, the same methods as in M14 are followed but with the following changes: the model
399 version is updated from 3.4.1 to 3.6, the CLM lake model is used in place of FLake, and no spin-
400 up procedure is employed for initialization of the lake model (initial LSTs are interpolated from
401 R2). As in M14, the Noah LSM (Chen and Dudhia, 2001) is used. Similar to the example shown
402 in Fig. 3, significant overestimation of ice coverage occurs during the first year (Fig. 4).

403 Although some adverse effects in this simulation are introduced due to the use of LSTs
404 interpolated from the coarse R2 data to provide an initial state, the similarity of these results to
405 FLake's fields in Fig. 3 suggests that the lack of spin-up time is a common problem to both
406 model runs. It is also implied by the methodologies of other CLM-based studies, which do use
407 spin-up or initialization procedures. Previous work by Subin et al. (2012) with the lake model in
408 CLM4 used a 110-year period for the spin-up of their reference simulation. In their experiments
409 with WRF-CLM, Gu et al. (2013) used an observed LST field for initialization. The 9 sub-
410 surface layers in their model were initialized based on the shape of an observed profile of lake
411 temperatures, valid during that period of the year and taken from Lake Superior. Using this
412 initialization methodology for a future downscaled simulation is not possible due to lack of
413 observations, but simulated future lake profiles could possibly be utilized for initialization of
414 downscaled runs. Overall, when using an embedded lake model in a downscaling application,
415 users should consider how the lake model is being initialized or spun-up in order to achieve
416 results with accuracy similar to the prior studies discussed above. If the lake state is initially
417 poorly prescribed from the GCM (with results similar to those shown in Fig. 2), a protracted
418 spin-up could be required to reach equilibrium with the driving fields in the RCM and obtain
419 more realistic results.

420
421 It has been noted previously that both WRF-FLake and WRF-CLM, as well as other 1-D lake
422 models, tend to exhibit difficulty in simulating deep lakes (e.g., Martynov et al., 2010;
423 Stepanenko et al., 2010; Gu et al., 2013; M14). Some model error can be attributed to the fact

424 that one-dimensional column models cannot represent 2- and 3-D processes (e.g., currents,
425 drifting ice, and formation of a thermal bar). While more sophisticated lake models could be
426 coupled with WRF, using computationally efficient 1-D models is advantageous in downscaling
427 applications, where computational resources are taxed by the use of finer resolution.
428 Additionally, Martynov et al. (2010) noted that more complex 3-D lake models are generally run
429 with much finer grid spacing (~ 2 km) than typical RCMs. Martynov et al. (2010) also compared
430 the simulated water temperatures and ice coverage from the Hostetler and FLake models, finding
431 that FLake generally performed better, but that the Hostetler model provides more opportunity to
432 improve model performance because it utilizes more vertical layers and is less reliant on
433 parameterization. A comparison of 1-D lake models by Thiery et al. (2014) showed favorable
434 results for both FLake and Hostetler-based models (including the lake model found in CLM4)
435 and noted their computational efficiency. When making regional climate projections with these
436 models it should be noted that both WRF-FLake and WRF-CLM assume that lake depths are
437 constant in time, which could be a poor assumption depending on the lake being modeled and the
438 future period. Also, more complex lake models may be appropriate for higher resolution (~ 2 km
439 grid spacing) RCM simulations focused on regions where lake dynamics are not adequately
440 captured by the column lake models discussed here.

441

442 **3 Conclusion**

443 It has been shown in the present study and in previous work (e.g., Gao et al., 2012; Bullock et al.,
444 2014; M14) that downscaling typically-coarse GCM data, using WRF's default interpolation
445 methods, to finer resolution WRF grids results in LST discontinuities and spurious ice formation
446 in the Great Lakes (Fig. 2). Although the default interpolation methods in WRF can easily be
447 modified to alter the interpolation scheme or to eliminate the search option, none of these simple
448 changes will overcome the challenges of setting the LSTs for inland water bodies that are not
449 resolved by driving data when WRF is used as a RCM. Various alternate methods have been
450 presented, and a summary of the positives and potential drawbacks to each approach is shown in
451 Table 2. Using WRF's "alternative" lake setting instead of the default interpolation method in
452 WPS eliminates unrealistically large and abrupt spatial discontinuities in temperature, but causes
453 large, deep lakes (such as Lake Superior) to erroneously freeze when ice is set based on an air-
454 temperature threshold. All the other approaches discussed above can simulate more realistic ice

455 cover than the default interpolation. However, the simulation of ice cover is obviously not a
456 factor in downscaling studies where the environment does not become sufficiently cold to
457 produce lake ice, such as those focusing on tropical regions. For example, the alternative lake
458 setting has been used to improve rainfall results (relative to the use of WRF's default
459 interpolation techniques) over Lake Victoria in Eastern Africa by Argent (2014). Using
460 climatological values in a future warmer climate will adversely affect results because LSTs
461 cannot be assumed to be stationary over time. A warming trend could be applied to observed
462 LST fields in order to improve this approach; however, a realistic trend may be complex to
463 derive for some lakes as Austin and Colman (2007) have shown an observed non-linear
464 amplification of warming LSTs relative to inland temperatures in the Great Lakes region. The
465 land mask alteration method of Gao et al. (2012) is effective at preventing discontinuities in
466 surface temperatures, but the use of temperatures from land grid cells in the GCM to set LSTs in
467 the RCM eliminates the presence of land-lake temperature contrasts which impact precipitation,
468 winds (i.e. land-sea breeze), and other near-surface fields. The use of a lake model (either
469 coupling a lake model to the RCM or using outputs from the GCM's lake model to drive the
470 RCM) can improve the representation of the lakes in retrospective simulations and has the ability
471 to simulate non-linear impacts of climate change on LSTs and ice cover (e.g., Gula and Peltier,
472 2012, M14).

473
474 For downscaling applications using WRF, we recommend setting LSTs and ice cover from either
475 a RCM- or GCM-driven lake model, especially when simulating mid-latitude regions. In their
476 studies focused on the Great Lakes, Notaro et al. (2013) and Wright et al. (2013) state that
477 accurate predictions of changes in LSTs and ice cover from lake models are needed when
478 simulating changes in regional climate. Zhao et al. (2012) also recommended the use of a lake
479 model for simulating changes in regional precipitation in the Great Lakes basin. Including
480 prognostic changes in the lake state is also possible if GCM data sets include predicted lake
481 surface temperatures and ice within their publicly-available outputs. For regional climate
482 modeling efforts in which the RCM data is being archived for various end-user applications, we
483 recommend the use of GCM- or RCM-driven lake modeling approaches. If such an approach is
484 not used, the potential adverse effects of setting LSTs and ice cover using interpolation from the
485 GCM should be documented, as is currently done in NARCCAP (2014).

486

487 The accuracy of the various approaches presented here is sensitive to the characteristics of the
488 lakes to which they are being applied. Approaches which set LSTs as a function of over-land
489 temperatures (such as the land mask modification approach or WRF's alternative lake setting)
490 may perform adequately when applied to smaller, shallower lakes where LST changes are more
491 closely coupled to air temperature changes. Investigators performing RCM experiments should
492 consider both the present-day interactions between the lake and overlying air masses as well as
493 the potential climate change impacts on the lakes within their model domain when choosing an
494 approach.

495

496 **4 Code availability**

497 WPS and the WRF model can be downloaded from
498 <http://www2.mmm.ucar.edu/wrf/users/downloads.html>. Source code for the FLake model can be
499 obtained at <http://www.flake.igb-berlin.de/sourcecodes.shtml>, and code needed to run the
500 coupled WRF-FLake model is available for download at
501 <http://web.atmos.ucla.edu/~gula/wrfflake>.

502 **Acknowledgements**

503 The lead author was supported by an appointment to the Research Participation Program at the
504 US Environmental Protection Agency (EPA) Office of Research and Development, administered
505 by the Oak Ridge Institute for Science and Education (ORISE). The WRF model is made
506 available by NCAR, funded by the National Science Foundation. Great Lakes ice cover data
507 were obtained from GLERL (<http://www.glerl.noaa.gov/data/pgs/glice/glice.html>). This research
508 has been subjected to the US EPA's administrative review and approved for publication. The
509 views expressed and the contents are solely the responsibility of the authors, and do not
510 necessarily represent the official views of the US EPA.

511 **References**

512 Anyah, R. O. and Semazzi, F. H. M.: Simulation of the sensitivity of Lake Victoria basin climate
513 to lake surface temperatures, *Theor. Appl. Climatol.*, 79, 55–69, 2004.

514

515 Argent, R. E.: Customisation of the WRF model over the Lake Victoria basin in east Africa,
516 M.S. thesis, North Carolina State University, Raleigh, NC, 124 pp., 2014.

517

518 Artale, V., Calmanti, S., Carillo, A., Dell’Aquila, A., Herrmann, M., Pisacane, G., Ruti, P. M.,
519 Sannino, G., Struglia, M. V., Giorgi, F., Bi, X., Pal, J. S., Rauscher, S., and The PROTHEUS
520 Group: An atmosphere–ocean regional climate model for the Mediterranean area: assessment of
521 a present climate simulation, *Clim. Dynam.*, 35, 721–740, 2010.

522

523 Asnani, G. C.: *Tropical Meteorology*, Vol. 1 and 2, Indian Institute of Tropical Meteorology
524 Pashan, Pune, 1012 pp., 1993.

525

526 Assel, R. A. and Robertson, D. M.: Changes in winter air temperatures near Lake Michigan,
527 1851–1993, as determined from regional lake-ice records, *Limnol. Oceanogr.*, 40, 165–176,
528 1995.

529

530 Austin, J. and Colman, S.: Lake Superior summer water temperatures are increasing more
531 rapidly than regional air temperatures: A positive ice–albedo feedback, *Geophys. Res. Lett.*, 34,
532 L06604, doi:10.1029/2006GL029021, 2007.

533

534 Bates, G. T., Giorgi, F., and Hostetler, S. W.: Toward the simulation of the effects of the Great
535 Lakes on regional climate, *Mon. Weather Rev.*, 123, 1505–1522, 1993.

536

537 Bullock, O. R., Alapaty, K., Herwehe, J. A., Mallard, M. S., Otte, T. L., Gilliam, R. C., and
538 Nolte, C. G.: An observation-based investigation of nudging in WRF for downscaling surface
539 climate information to 12 km grid spacing, *J. Appl. Meteorol. Clim.*, 53, 20–33, 2014.

540

541 Burnett, A. W., Kirby, M. E., Mullins, H. T., and Patterson, W. P.: Increasing Great Lake–effect
542 snowfall during the twentieth century: a regional response to global warming?, *J. Climate*, 16,
543 3535–3542, 2003.

544

545 Cairns, M. M., Collins, R., Cylke, T., Deutschendorf, M., and Mercer, D.: A lake effect snowfall
546 in western Nevada. Part I: Synoptic setting and observations, Preprints, 18th Conf. on Weather
547 Analysis and Forecasting, Fort Lauderdale, FL, 29 July 2001, *Am. Meteor. Soc.*, 329–332, 2001.

548

549 Carpenter, D. M.: The lake effect of the Great Salt Lake: overview and forecast problems,
550 *Weather Forecast.*, 8, 181–193, 1993.

551

552 Chen, F. and Dudhia, J.: Coupling and advanced land surface–hydrology model with the Penn
553 State–NCAR MM5 modeling system, Part I: Model implementation and sensitivity, *Mon.*
554 *Weather Rev.*, 129, 569–585, 2001.

555

556 Feser, F., Rockel, B., von Storch, H., Winterfeldt, J., and Zahn, M.: Regional climate models add
557 value to global model data: a review and selected examples. *B. Am. Meteorol. Soc.*, 92, 1181–
558 1192, 2011.

559

560 Gao, Y., Fu, J. S., Drake, J. B., Liu, Y., and Lamarque, J.-F.: Projected changes of extreme
561 weather events in the eastern United States based on a high resolution climate modeling system,
562 *Environ. Res. Lett.*, 7, 044025, doi:10.1088/1748-9326/7/4/044025, 2012.

563

564 Gerbush, M. R., Kristovich, D. A. R., and Laird, N. F.: Mesoscale boundary layer and heat flux
565 variations over pack ice–covered Lake Erie, *J. Appl. Meteorol. Clim.*, 47, 668–682, 2008.

566

567 Gu, H., Jin, J., Wu, Y., Ek, M., and Subin, Z.: Calibration and validation of lake surface
568 temperature simulations with the coupled WRF-lake model, *Clim. Chang.*, doi: 10.1007/s10584-
569 013-0978-y, in press, 2013.

570

571 Gualdi, S., Somot, S., Li, L., Artale, V., Adani, M., Bellucci, A., Braun, A., Calmanti, S., Carillo,
572 A., Dell'Aquila, A., Déqué, M., Dubois, C., Elizalde, A., Harzallah, A., Jacob, D., L'Hévéder,
573 B., May, W., Oddo, P., Ruti, P., Sanna, A., Sannino, G., Scoccimarro, E., Sevault, F., and
574 Navarra, A.: The CIRCE simulations: Regional climate change projections with realistic
575 representation of the Mediterranean Sea, *B. Am. Meteorol. Soc.*, 94, 65–81, 2013.
576

577 Gula, J. and Peltier, W. R.: Dynamical downscaling over the Great Lakes basin of North
578 America using the WRF regional climate model: the impact of the Great Lakes system on
579 regional greenhouse warming, *J. Climate*, 25, 7723–7742, 2012.
580

581 Hostetler, S. W. and Bartlein, P. J.: Simulation of lake evaporation with application to modeling
582 lake level variations of Harney-Malheur Lake, Oregon, *Water Resour. Res.*, 26, 2603–2612,
583 1990.
584

585 Hostetler, S. W., Bates, G. T., and Giorgi, F.: Interactive coupling of a lake thermal model with a
586 regional climate model, *J. Geophys. Res.*, 98, 5045–5057, 1993.
587

588 Hostetler, S. W., Giorgi, F., Bates, G. T., and Bartlein, P. J.: Lake-atmosphere feedbacks
589 associated with paleolakes Bonneville and Lahontan, *Science*, 263, 665–668, 1994.
590

591 Huggins, A. W., Kingsmill, D. E., and Cairns, M. M.: A lake effect snowfall in western Nevada–
592 Part II: Radar characteristics and quantitative precipitation estimates, Preprints, 18th Conf. on
593 Weather Analysis and Forecasting, Fort Lauderdale, FL, 29 July 2001, *Amer. Meteor. Soc.*, 333
594 337, 2001.
595

596 Kanamitsu, M., Ebisuzaki, W., Woollen, J., Yang, S.-K., Hnilo, J. J., Fiorino, M., and Potter, G.
597 L.: NCEP–DOE AMIP-II Reanalysis (R-2). *B. Am. Meteorol. Soc.*, 83, 1631–1643, 2002.
598

599 Kourzeneva, E., Samuelsson, P., Ganbat, G., and Mironov, D.: Implementation of Lake Model
600 FLake into HIRLAM, *HIRLAM Newsletter* 54, 54–64, available from HIRLAM-A Programme,

601 c/o J. Onvlee, KNMI, P. O. Box 201, 3730 AE De Bilt, the Netherlands, available at: [http:](http://hirlam.org)
602 [//hirlam.org](http://hirlam.org) (last access: 20 October 2014), 2008.
603
604 Kunkel, K. E., Ensor, L., Palecki, M., Easterling, D., Robinson, D., Hubbard, K. G., and
605 Redmond, K.: A new look at lake-effect snowfall trends in the Laurentian Great Lakes using a
606 temporally homogeneous data set, *J. Great Lakes Res.*, 35, 23–29, 2009.
607
608 Laird, N. F., Desrochers, J., and Payer, M.: Climatology of lake-effect precipitation events over
609 Lake Champlain, *J. Appl. Meteorol. Clim.*, 48, 232–250, 2009.
610
611 Magnuson, J. J., Robertson, D. M., Benson, B. J., Wynne, R. H., Livingstone, D. M., Arai, T.,
612 Assel, R. A., Barry, R. G., Card, V., Kuusisto, E., Granin, N. G., Prowse, T. D., Stewart, K. M.,
613 and Vuglinski, V. S.: Historical trends in lake and river ice cover in the Northern Hemisphere,
614 *Science*, 289, 1743–1746, 2000.
615
616 Mallard, M. S., Nolte, C. G., Bullock, O. R., Spero, T. L., and Gula, J.: Using a coupled lake
617 model with WRF for dynamical downscaling, *J. Geophys. Res.*, 119, 7193–7208,
618 doi:10.1002/2014JD021785, 2014.
619
620 Martynov, A., Laprise, R., and Sushama, L.: Off-Line lake water and ice simulations: a step
621 towards the interactive lake coupling with the Canadian Regional Climate Model, *Geophysical*
622 *Research Abstracts*, Vol. 10, EGU2008-A-02898, EGU General Assembly 2008, Vienna,
623 Austria, 2008.
624
625 Martynov, A., Sushama, L., and Laprise, R.: Simulation of temperate freezing lakes by one-
626 dimensional lake models: performance assessment for interactive coupling with regional climate
627 models, *Boreal Environ. Res.*, 15, 143–164, 2010.
628
629 Mearns, L. O., Arritt, R., Biner, S., Bukovsky, M. S., McGinnis, S., Sain, S., Caya, D., Correia
630 Jr., J., Flory, D., Gutowski, W., Takle, E. S., Jones, R., Leung, R., Moufouma-Okia, W.,
631 McDaniel, L., Nunes, A. M. B., Qian, Y., Roads, J., Sloan, L., and Snyder, M.: The North

632 American regional climate change assessment program: overview of phase I results, B. Am.
633 Meteorol. Soc., 93, 1337–1362, 2012.

634

635 Mironov, D. V.: Parameterization of lakes in numerical weather prediction. Description of a lake
636 model, COSMO Technical Report, No. 11, Deutscher Wetterdienst, Offenbach am Main,
637 Germany, 41 pp., 2008.

638

639 Mironov, D., Heise, E., Kourzeneva, E., Ritter, B., Schneider, N., and Terzhevik, A.:
640 Implementation of the lake parameterization scheme FLake into the numerical weather
641 prediction model COSMO, Boreal Env. Res., 15, 218–230, 2010.

642

643 NARCCAP: Caveats for Users, available at: <http://www.narccap.ucar.edu/about/caveats.html>,
644 last access: 11 August 2014.

645

646 Notaro, M., Holman, K., Zarrin, A., Fluck, E., Vavrus, S., and Bennington, V.: Influence of the
647 Laurentian Great Lakes on regional climate, J. Climate, 26, 789–804, 2013.

648

649 Oleson, K. W., Lawrence, D. M., Bonan, G. B., Flanner, M. G., Kluzek, E., Lawrence, P. J.,
650 Levis, S., Swenson, S. C., Thornton, P. E., Dai, A., Decker, M., Dickinson, R., Feddema, J.,
651 Heald, C. L., Hoffman, F., Lamarque, J.-F., Mahowald, N., Niu, G.-Y., Qian, T., Randerson, J.,
652 Running, S., Sakaguchi, K., Slater, A., Stöckli, R., Wang, A., Yang, Z.-L., Zeng, X., and Zeng,
653 X.: Technical description of version 4.0 of the Community Land Model (CLM), National Center
654 for Atmospheric Research, P.O. Box 3000, Boulder, Colorado 80307, USA, NCAR/TN-
655 478+STR, 2010.

656

657 Oleson, K. W., Lawrence, D. M., Bonan, G. B., Drewniak, B., Huang, M., Koven, C. D., Levis,
658 S., Li, F., Riley, W. J., Subin, Z. M., Swenson, S. C., Thornton, P. E., Bozbiyik, A., Fisher, R.,
659 Heald, C. L., Kluzek, E., Lamarque, J.-F., Lawrence, P. J., Leung, L. R., Lipscomb, W.,
660 Muszala, S., Ricciuto, D. M., Sacks, W., Sun, Y., Tang, J., and Yang, Z.-L.: Technical
661 description of version 4.5 of the Community Land Model (CLM), National Center for

662 Atmospheric Research, P.O. Box 3000, Boulder, Colorado 80307, USA, NCAR Technical Note
663 NCAR/TN-503+STR, 420 pp., doi:10.5065/D6RR1W7M, 2013.
664

665 Ratnam, J. V., Filippo, G., Kaginalkar, A., and Cozzini, S.: Simulation of the Indian monsoon
666 using the RegCM3-ROMS regional coupled model, *Clim. Dynam.*, 33, 119–139, 2009. Rinke,
667 A., Gerdes, R., Dethloff, K., Kandlbinder, T., Karcher, M., Kauker, F., Frickenhaus, S., Köberle,
668 C., and Hiller, W.: A case study of the anomalous Arctic sea ice conditions during 1990: insights
669 from coupled and uncoupled regional climate model simulations, *J. Geophys. Res.*, 108, 4275,
670 doi:10.1029/2002JD003146, 2003.
671

672 Samuelsson, P., Kourzeneva, E., and Mironov, D.: The impact of lakes on the European climate
673 as simulated by a regional climate model, *Boreal Env. Res.*, 15, 113–129, 2010.
674

675 Schultz, D. M., Arndt, D. S., Stensrud, D. J., and Hanna, J. W.: Snowbands during the cold-air
676 outbreak of 23 January 2003, *Mon. Weather Rev.*, 132, 827–842, 2004.
677

678 Scott, R. W. and Huff, F. A.: Impacts of the Great Lakes on regional climate conditions, *J. Great
679 Lakes Res.*, 22, 845–863, 1996.
680

681 Skamarock, W. C. and Klemp, J. B.: A time-split nonhydrostatic atmospheric model for weather
682 research and forecasting applications, *J. Comp. Phys.*, 227, 3465–3485, 2008.
683

684 Skamarock, W. C., Klemp, J. B., Dudhia, J., Gill, D. O., Barker, D. M., Duda, M., Huang, X.-Y.,
685 Wang, W., and Powers, J. G.: A description of the Advanced Research WRF version 3, Tech.
686 Rep., National Center for Atmospheric Research, P.O. Box 3000, Boulder, Colorado 80307,
687 USA, NCAR/TN-475+STR, 113 pp., 2008.
688

689 Steenburgh, W. J. and Onton, D. J.: Multiscale analysis of the 7 December 1998 Great Salt
690 Lake–effect snowstorm, *Mon. Weather Rev.*, 129, 1296–1317, 2001.
691

692 Stepanenko, V. M., Goyett, S., Martynov, A., Perroud, M., Fang, X., and Mironov, D.: First
693 steps of the Lake Model Intercomparison Project: LakeMIP, *Boreal Env. Res.*, 15, 191–202,
694 2010.

695

696 Subin, Z. M., Riley, W. J., and Mironov, D.: An improved lake model for climate simulations:
697 Model structure, evaluation, and sensitivity analyses in CESM1, *J. Adv. Model. Earth Syst.*, 4,
698 M02001, doi:10.1029/2011MS000072, 2012.

699

700 Tardy, A.: Lake-effect and lake-enhanced snow in the Champlain Valley of Vermont, Tech.
701 Memo. 2000-05, NWS Eastern Region, 27 pp., Burlington, Vermont, USA, 2000.

702

703 Thiery, W., Stepanenko, V. M., Fang, X., Johnk, K. D., Li, Z., Martynov, A., Perroud, M., Subin,
704 Z. M., Darchambeau, F., Mironov, D. and van Lipzig, N. P. M.: LakeMIP Kivu: evaluating the
705 representation of a large, deep tropical lake by a set of one-dimensional lake models, *Tellus*, 66,
706 21390, 2014.

707

708 Wang, J., Bai, X., Hu, H., Clites, A., Colton, M., and Lofgren, B.: Temporal and spatial
709 variability of Great Lakes ice cover, 1973–2010, *J. Climate*, 25, 1318–1329, 2012a.

710

711 Wang, J., Assel, R. A., Walterscheid, S., Clites, A. H., and Bai, X.: Great Lakes ice climatology
712 update: winter 2006–2011 description of the digital ice cover data set, NOAA Technical
713 Memorandum GLERL-155, 37 pp., Ann Arbor, Michigan, USA, 2012b.

714

715 Wilken, G. R.: A lake-effect snow in Arkansas, NWS Southern Region, Tech. Attachment
716 SR/SSD 97-21, 5 pp., Little Rock, Arkansas, USA, 1997.

717

718 Wilson, J. W.: Effect of Lake Ontario on precipitation, *Mon. Weather Rev.*, 105, 207–214, 1977.

719

720 WRF User’s Guide: User’s Guide for the Advanced Research WRF (ARW) Modeling System
721 Version 3.6, available at:

722 http://www2.mmm.ucar.edu/wrf/users/docs/user_guide_V3/ARWUsersGuideV3.pdf, last access:
723 12 June 2014.
724
725 Wright, D. M., Posselt, D. J., and Steiner, A. L.: Sensitivity of lake-effect snowfall to lake ice
726 cover and temperature in the Great Lakes region, *Mon. Weather Rev.*, 141, 670–689, 2013.
727
728 Zhao, L., Jin, J., Wang, S.-Y., and Ek, M. B.: Integration of remote-sensing data with WRF to
729 improve lake-effect precipitation simulations over the Great Lakes region, *J. Geophys. Res.*, 117,
730 D09102, doi:10.1029/2011JD016979, 2012.
731
732 Zulauf, M. A. and Kreuger, S. K.: Two-dimensional cloud-resolving modeling of the
733 atmospheric effects of Arctic leads based upon midwinter conditions at the surface heat budget
734 of the Arctic Ocean ice camp, *J. Geophys. Res.*, 108, 4312, doi:10.1029/2002JD002643, 2003.
735

736 Table 1. List of WRF versions discussed in the text, ordered chronologically by the date of
 737 release and with relevant model updates summarized.

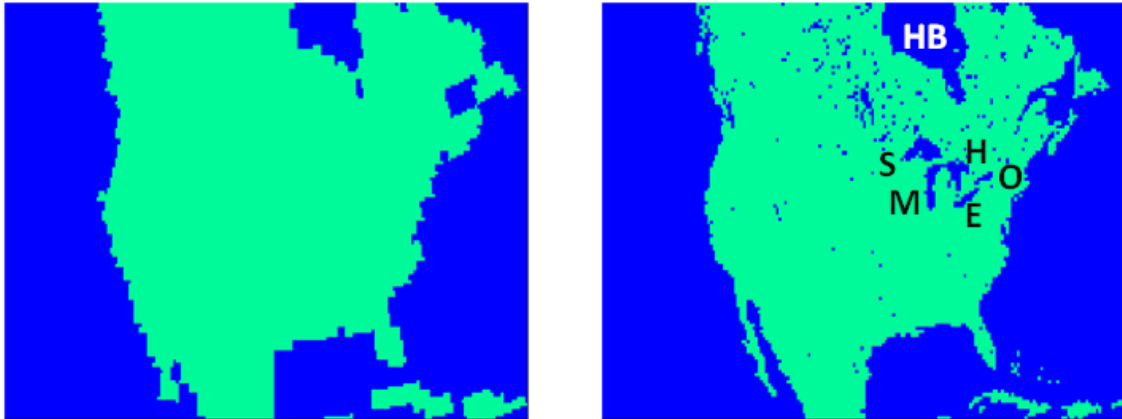
WRF version	Released	Updates of Interest
3.3	April 2011	“Alternative initialization of lake SSTs” option included in WPS so users can set LSTs from temporally averaged 2 m temperatures.
3.5	April 2013	CLM available as an LSM within WRF, but with its lake model disabled.
3.5.1	September 2013	Default surface water temperature at which WRF prescribes ice (“seaice_threshold”) is lowered from 271 K to 100 K.
3.6	April 2014	CLM lake model available with any choice of LSM. Lake depths can be prescribed as a constant or as a spatially varying 2-D field.

738

739 Table 2. A summary of the pros and cons of each method of treating lake surface temperatures
 740 and ice coverage described in the text. All approaches were found to eliminate unrealistic
 741 temperature discontinuities resulting from WRF's default interpolation methods as shown in Fig.
 742 2.

Methodology	Positives	Potential drawbacks
WRF's Alternative Lake Setting	Effective at representing LSTs when lake temperatures are closely coupled with atmospheric temperatures.	Unrealistic ice formation possible when 2 m temperatures are below freezing. Cannot account for varying lake depths and differing timescales of warming and cooling throughout lakes.
Climatological	Observed LSTs and ice taken from high resolution analyses.	For long-term simulations, user must include temperature trend or LSTs will not be in equilibrium with future climate state. Does not represent interannual variability of lake state.
Land Mask Modification	Future LSTs can be taken from projected GCM temperatures.	Eliminates land-lake temperature contrasts.
Lake Model Component	Models have ability to simulate future changes in LST and ice.	Additional preprocessing needed to provide lake model spin-up for RCM run or to use lake fields simulated by GCM.

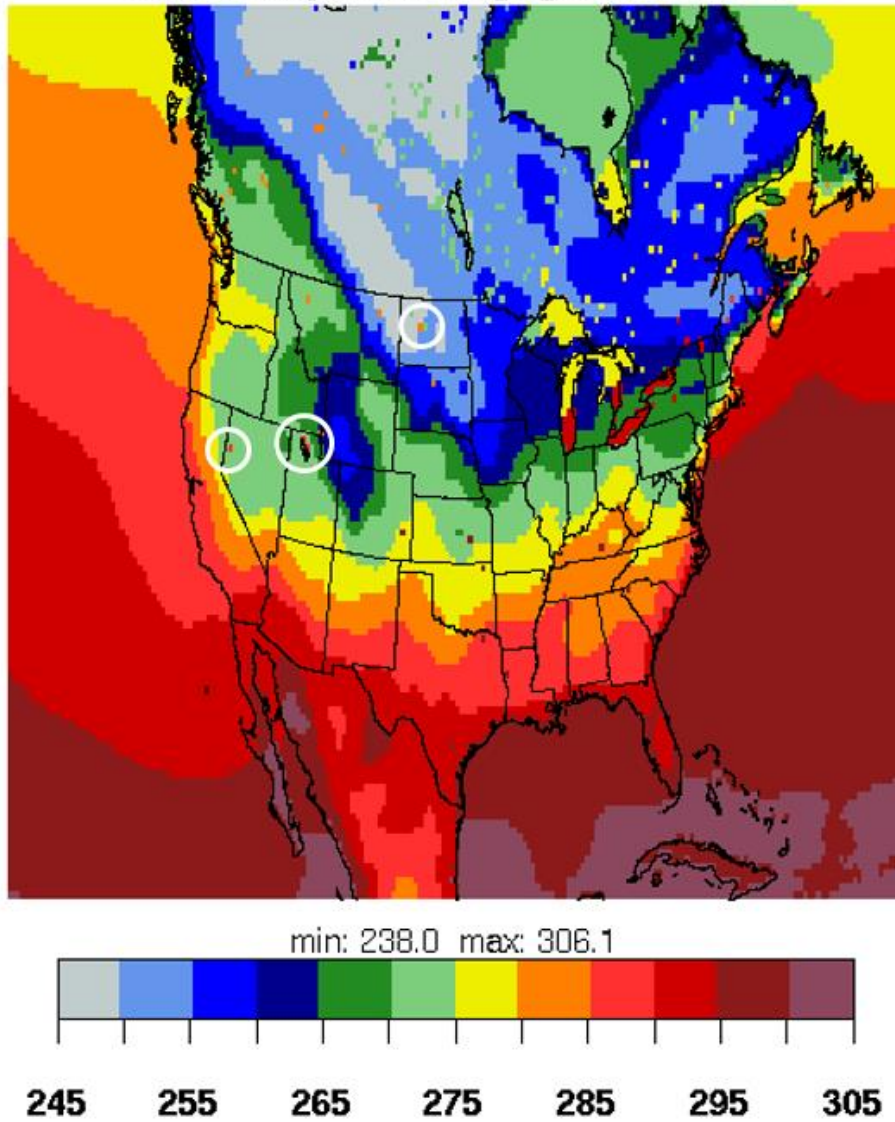
743



744

745 Figure 1. The ocean mask from the 1⁰ CESM data (which is used by WPS to determine the
746 locations of land and water points from CESM), as shown in the area corresponding to a WRF
747 36-km continental US domain (left), and the 36 km WRF grid's land-water mask (right). Labels
748 are placed to indicate the locations of Lakes Superior ("S"), Michigan ("M"), Huron ("H"), Erie
749 ("E") and Ontario ("O"), as well as Hudson Bay ("HB").

Skin Temperature [K] 1994-12-01

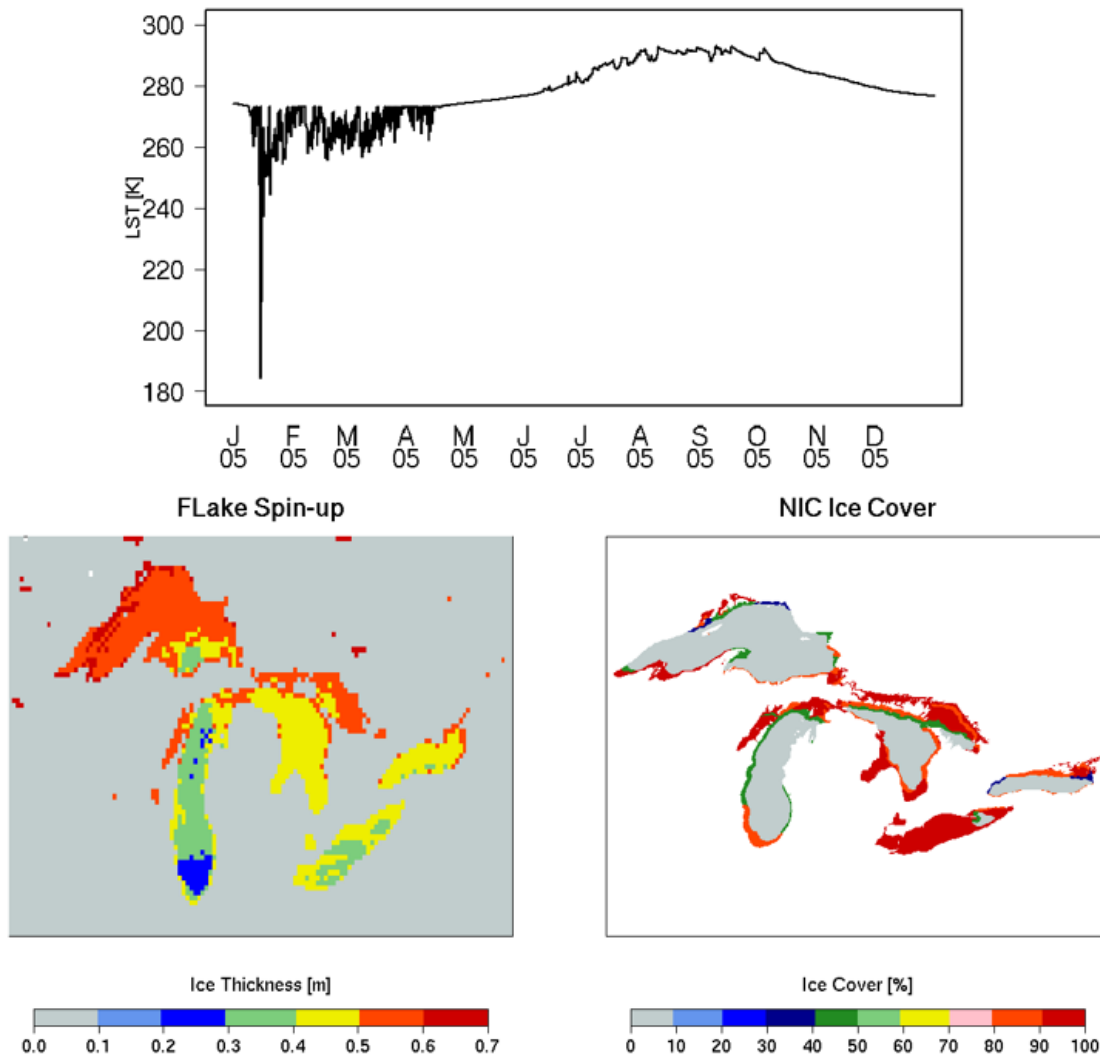


750

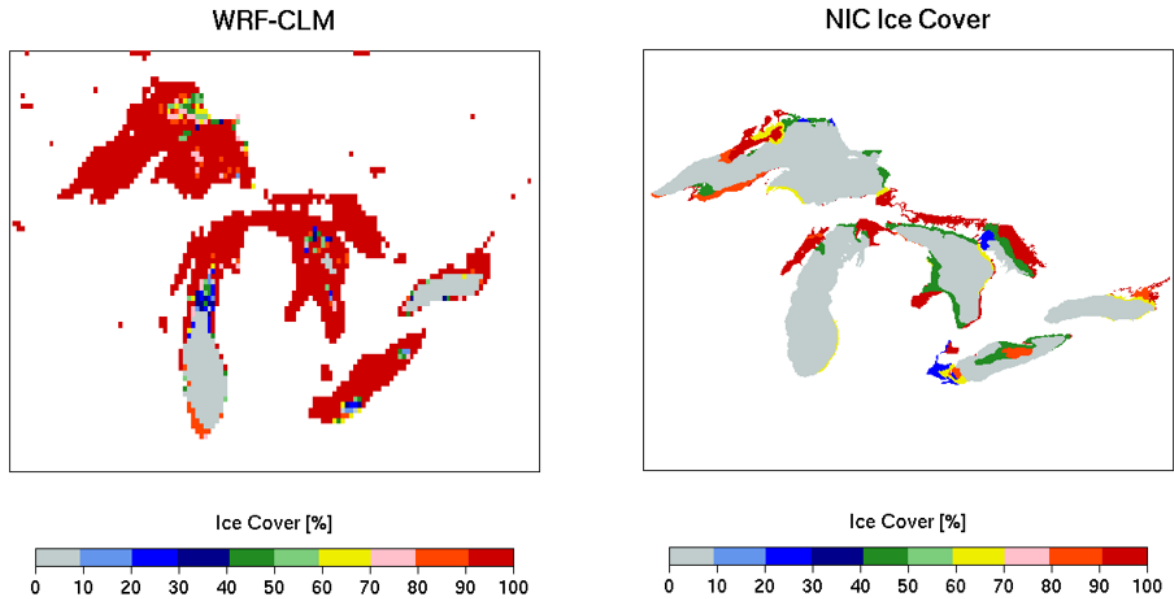
751 Figure 2. The skin temperature (K) processed from CESM to the 36-km WRF grid using WPS

752 and valid at 00 UTC 1 Dec 1994. White circles indicate the locations of Pyramid Lake, Great

753 Salt Lake, and Lake Sakakawea, from west to east, respectively.



754
 755 Figure 3. Surface temperature from the initial year of a 10-year FLake spin-up simulation, taken
 756 from a point near the north shore of Lake Superior (48.47° N, 87.54° W) and shown hourly from
 757 1 January to 31 December 2005 (top). LSTs at all lake cells are initialized with a default value
 758 of 274.15 K, and the time series shows either ice or water surface temperatures depending on
 759 whether ice is present. Simulated ice thickness (m) taken from day 30 of the same FLake
 760 simulation, valid 30 January 2005 (bottom left). Fractional ice values observed on this date
 761 plotted from the NIC ice analysis (bottom right).



762
 763 Figure 4. Simulated ice cover (%) taken from a WRF simulation (valid 2 March 2006, after ~ 4
 764 months of simulation time) with the same model configuration as described in M14, but
 765 simulated with WRF version 3.6 and the use of the CLM lake model in place of FLake (left). A
 766 2-D field of lake depths (instead of a single default value) were used from WPS to set the lake
 767 depth in this simulation. Ice coverage observed on this date is plotted from the NIC ice analysis
 768 (right).